

# Magnetic Trapping of Metastable Calcium Atoms

Dirk P. Hansen,\* Janis R. Mohr, and Andreas Hemmerich

*Institut für Laser-Physik, Universität Hamburg, Jungiusstrasse 9, D-20355 Hamburg, Germany*

(Dated: October 30, 2018)

Metastable calcium atoms, produced in a magneto-optic trap (MOT) operating within the singlet system, are continuously loaded into a magnetic trap formed by the magnetic quadrupole field of the MOT. At MOT temperatures of 3 mK and 240 ms loading time we observe  $1.1 \times 10^8$  magnetically trapped  $^3P_2$  atoms at densities of  $2.4 \times 10^8 \text{ cm}^{-3}$  and temperatures of 0.61 mK. In a modified scheme we first load a MOT for metastable atoms at a temperature of 0.18 mK and subsequently release these atoms into the magnetic trap. In this case 240 ms of loading yields  $2.4 \times 10^8$  trapped  $^3P_2$  atoms at a peak density of  $8.7 \times 10^{10} \text{ cm}^{-3}$  and a temperature of 0.13 mK. The temperature decrease observed in the magnetic trap for both loading schemes can be explained only in part by trap size effects.

PACS numbers: 32.80.Pj, 42.50.Vk, 42.62.Fi, 42.50.-p

Earth alkaline atoms provide a unique combination of interesting spectroscopic features connected to their two valence electrons which give rise to singlet and triplet excitations. The singlet systems possess strong principle fluorescence lines well suited for laser cooling with remarkable efficiency. Yet, temperatures are limited to the mK domain, due to the absence of ground state Zeeman structure, a prerequisite for sub-Doppler techniques. The triplet systems, however, have readily accessible narrow band optical transitions that render possible refined laser cooling schemes with the promise of temperatures even beyond the microkelvin range. In fact, such schemes have recently been experimentally realized for strontium and calcium [1, 2, 3, 4]. Owing to their spectroscopic peculiarities such ultracold earth alkaline samples open up new prospects for ultraprecise atomic clocks [5, 6, 7] and cold collision studies which allow direct comparisons with ab initio theoretical calculations [8, 9, 10]. The formation of Bose-Einstein condensates (BEC, [11]) for this exciting group of atoms appears particularly desirable.

A key technique for obtaining BEC in alkalis and noble gases has been magnetic trapping. This trapping technique outperforms optical techniques in two ways. It provides well controllable potential wells with sufficient steepness. The regime of high elastic collision rates, a precondition for efficient evaporative cooling, is thus easily accessible. Secondly, the presence of antibinding magnetic sublevels allows to actively force evaporation in a particular effective way by selectively expelling energetic atoms from the trap. The extension of this successful trapping technique to earth alkaline atoms may pave the route to BEC in this atom group. While the singlet ground state of these species lacks magnetic substructure, the ground state of the triplet system typically offers a particularly large Zeeman effect. Specifically, the long-lived  $^3P_2, m_J=2$  state appears appropriate for mag-

netic trapping and the formation of BEC. Recent calculations for calcium and strontium predict a positive scattering length (and thus stable BEC) for this state [10].

In this article we explore the application of magnetic trapping to the case of  $^{40}\text{Ca}$ . We demonstrate loading of a magnetic quadrupole trap with several times  $10^8$  calcium atoms in the  $^3P_2$  metastable state at peak densities near  $10^{11} \text{ cm}^{-3}$  and temperatures around 0.13 mK. We prepare cold Calcium  $^3P_2$  atoms in the mK range at very high rates from a magneto-optic trap operating on the principle fluorescence line of the singlet system at 423 nm (called SMOT in the following) [12]. The excited state of the SMOT-transition has a small decay channel leading to the  $^1D_2$  state ( $\gamma_1 = 2180 \text{ s}^{-1}$  [13]) and further on to the  $^3P_2$  ( $\gamma_2 = 96 \text{ s}^{-1}$ ) and  $^3P_1$  ( $\gamma_3 = 300 \text{ s}^{-1}$ ) triplet states (see Fig.1a for relevant Ca levels). While the atoms decaying via  $^3P_1$  return to the ground state in about 3 ms and can be recycled into the SMOT, those decaying to  $^3P_2$  represent a permanent loss that limits the SMOT life time to 21 ms. Transfer rates into the  $^3P_2$  state can exceed  $10^{10}$  atoms/s at a temperature of about 2–3 mK determined by the Doppler temperature of the SMOT. In order to prepare even colder  $^3P_2$  atoms, we superimpose a second magneto-optic trap (TMOT) for  $^3P_2$  atoms using the narrow-band  $^3P_2 \rightarrow ^3D_3$  triplet transition at 1978 nm [4]. If the TMOT is optimized for high loading rates it typically collects several times  $10^8$  atoms within 240 ms at temperatures around 180  $\mu\text{K}$ .

The magnetic quadrupole field shared by the SMOT and TMOT provides a natural test ground for magnetic trapping of  $^3P_2$  atoms as has been recently discussed in detail in ref. [14]. The trapping potential is given by  $U(x, y, z) = U_0 \sqrt{\frac{1}{4}(x^2 + y^2) + z^2}$  with  $U_0 = 2\pi\hbar \times g \times m_J \times b \times (1.4 \text{ MHz/Gauss})$ , where  $b$  is the magnetic field gradient,  $m_J$  is the magnetic quantum number, and  $g$  denotes the g-factor. Due to the large value  $g=3/2$  for the  $^3P_2$  state, for atoms in the low field seeking  $m_J=2$  Zeeman component a magnetic field gradient  $b$  of only 2.5 Gauss/cm is sufficient to compensate for gravity, and 10 Gauss/cm provide a significant trap

\*Electronic address: dhansen@physnet.uni-hamburg.de

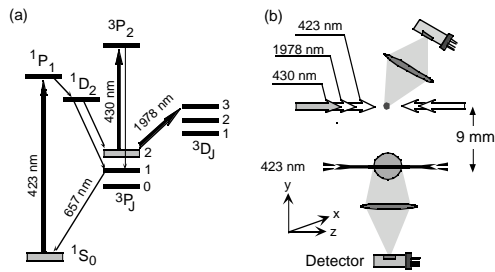


FIG. 1: (a) Relevant energy levels and transitions in  $^{40}\text{Ca}$ . (b) Sketch of the experimental setup. SMOT and TMOT beams are indicated only in the  $z$ -direction.

potential of 2.5 mK/cm.

The experimental setup is an extension of that used in ref. [4]. Fig.1b provides a sketch of the relevant elements. Three beams with 8 mm in diameter and 20 mW power, detuned from resonance by two times the natural line width, are retroreflected in order to form the SMOT. Atoms are provided from a Zeeman-decelerated atomic beam. By observation of the 423 nm fluorescence we measure  $4 \times 10^7$  atoms in the excited  $^1P_1$  state of the SMOT. From the known transition rates (see e.g. ref. [13]) we can deduce a transfer rate into the  $^3P_2$  state of  $1.9 \times 10^{10}$  atoms/s. The magnetic quadrupole field with horizontal symmetry axis ( $z$ -axis) has a trap depth of 20.6 mK and a magnetic field gradient (along the  $z$ - axis) of  $b=26$  Gauss/cm in the origin. For monitoring the operation of the SMOT we record the fluorescence at 657 nm due to atoms decaying via  $^1D_2$  and  $^3P_1$  back to the ground state. In order to observe the  $^3P_2$  atoms we optically pump them to the  $^3P_1$  state by applying a 0.5 ms pulse of 430 nm light resonant with the  $^3P_2(4s4p) \rightarrow ^3P_2(4p4p)$  transition. The  $1/e^2$ -radius of this optical pumping beam is 3 mm. In order to work with a reduced optical pumping volume, a variable aperture placed inside this beam is imaged onto the atomic sample. The  $^3P_1$  atoms decay to the  $^1S_0$  singlet ground state in 0.4 ms and are subject to ballistic expansion. Temperature measurements are performed with a time of flight method (TOF). A 10 mm wide and 0.5 mm thick sheet of light resonant with the  $^1S_0 \rightarrow ^1P_1$  transition is placed 9 mm below the center of the optical pumping beam (see Fig.1b). The fluorescence in this light sheet is recorded by a photo multiplier from below. Because we operate the TMOT with the same magnetic quadrupole field, the narrow bandwidth (57 kHz) of the  $^3P_2 \rightarrow ^3D_3$  transition is power-broadened to a peak value of 16 MHz, in order to obtain sufficient spatial capture volume. With 5 mW for each of the three retroreflected beams of 10 mm diameter the resonant peak saturation parameter is  $7.6 \times 10^4$ .

In Fig.2 the operation of the magnetic trap is illustrated. Before  $t=0$ , for about 240 ms atoms are Zeeman cooled, loaded into the SMOT, and transferred to

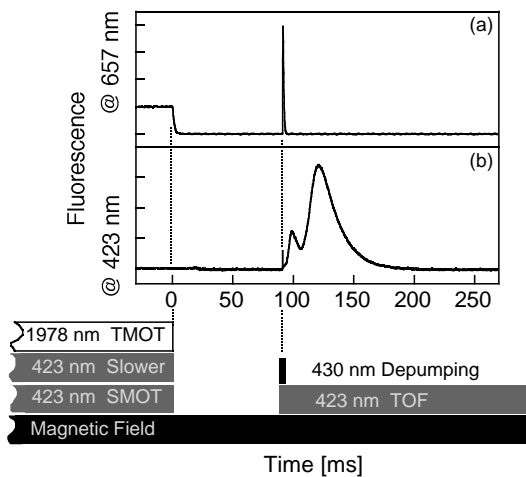


FIG. 2: Typical experimental sequence comprised of a 240 ms loading phase ( $t < 0$ ), a variable phase of magnetic trapping, and a TOF phase initiated by a 0.5 ms optical pumping pulse at 430 nm. The fluorescence at 657 nm (a) and a TOF signal (b) are shown.

the magnetically trapped  $^3P_2$  state. At  $t=0$  the 423 nm beams are disabled, i.e. no further loading of the magnetic trap occurs which is seen from the drop of 657 nm fluorescence in trace (a). After a variable time delay the optical pumping pulse is applied which gives rise to a spike of 657 nm fluorescence, and a TOF spectrum is recorded (trace (b)). Alternatively, during the loading period before  $t=0$  we may apply the TMOT. In this case the magnetic trap is not continuously loaded but at  $t=0$  the  $^3P_2$  atoms trapped and cooled in the TMOT are suddenly released into the magnetic trap. Detection is performed as in the case of SMOT loading. While TMOT loading allows for lower initial temperatures, an attractive feature of SMOT loading is its continuous character, i.e. the possibility to add particles to the trap without disturbing those already trapped, as recently discussed in ref. [14] and demonstrated for chromium atoms in ref. [15].

By varying the trapping time in Fig.2 and observing the size of the 657 nm fluorescence peak in trace (a) we can measure the life time of the magnetic trap. The case of TMOT loading is shown in Fig.3a (open rectangles). For comparison, the filled rectangles show the decay of the TMOT itself. A surprisingly high transfer efficiency of about 75 % is observed. The fitted exponentials (solid lines in Fig.3a) correspond to a model which neglects two-body collision losses. The decay time constants of  $239 \pm 4$  ms in the upper trace and  $229 \pm 8$  ms in the lower trace agree within the errors and are in accordance with the  $10^{-8}$  mbar vacuum conditions. For SMOT loading the same decay time is found. Although a model accounting for inelastic two-body collisions yields slightly better fits for the lower trace in Fig.3a, slow fluctuations of the initial sample sizes in our present data do not allow us to extract reliable values for the collision rate.

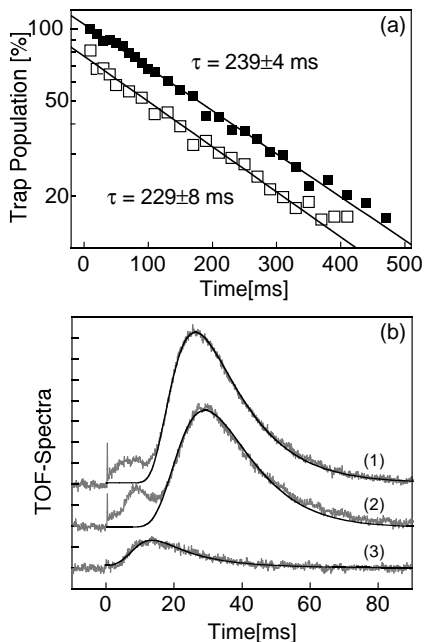


FIG. 3: (a) Life time measurement of the magnetic trap for TMOT loading (open rectangles) and the TMOT for comparison (filled rectangles). The solid lines show exponential fits. (b) TOF spectra (grey color) and corresponding theoretical fits (black lines) for the TMOT (1) and the magnetic trap for TMOT loading (2) and SMOT loading (3) respectively. All traces share the same scale.

In Fig.3b TOF spectra are shown for three different cases. The upper trace (1) shows a TOF spectrum for atoms trapped in the TMOT for 370 ms with a loading period of 240 ms. In trace (2) the TMOT was loaded for 240 ms but subsequently the atoms were released into the magnetic trap and held there for 130 ms. In trace (3) the SMOT continuously loaded the magnetic trap for 240 ms followed by 130 ms without further loading. Note that in either case (2) and (3) the temperature found in the magnetic trap is significantly lower than that of the loaded atomic sample. In trace (3) the initial sample in the SMOT has a temperature of about 3 mK, while that of the magnetically trapped sample is only 611  $\mu$ K. In (2) the initial sample temperature is 182  $\mu$ K as seen in trace (1), while the temperature in the magnetic trap is only 134  $\mu$ K. The fits in Fig.3b (solid black lines) used to evaluate temperatures are derived from a TOF model with three fit parameters: the initial vertical diameters and atom numbers of the fraction of atoms participating in the ballistic flight, and the temperatures. The initial sizes found in these fits are consistent with those observed. The diameter of the TMOT is estimated to be 2 mm by scanning the 430 nm optical pumping beam with 0.5 mm diameter through the atomic sample and observing the 657 nm fluorescence peak of Fig.2a. This corresponds to the best fit in trace (1) obtained for 2.4 mm. The initial diameter for the TOF measurement of trace (2) is estimated similarly to be about 4 mm correspond-

ing to the value of 4.1 mm in the best fit. The best fit value of the initial diameter for trace (3) of 7.9 mm does not reflect the size of the trapped population but is determined by the 3 mm maximal radius of the optical pumping beam. In traces (2) and (3) we also recognize a hot fraction of atoms occurring at early times in the TOF-spectra which are not accounted for in our model. Particularly, in the case of TMOT loading (trace (2)) a well distinguished hot fraction (at several mK) is visible. For TMOT loading, TOF spectra recorded for trapping times shorter than 100 ms show additional structure which reflects non-equilibrium trap dynamics as is illustrated in Fig.4. The initial sharp peaks, resulting from the 430 nm depumping photons, indicate the release of the atoms from the magnetic trap. One recognizes an oscillation of population between hotter and colder fractions of atoms occurring at earlier or later times in the TOF spectra.

In order to explain the temperature decrease in the magnetic trap we first consider the case of SMOT loading in trace (3). The  $^3P_2$  trap potential is continuously loaded by the cold flux of atoms emerging from the trapping volume of the SMOT with  $\sigma=1$  mm  $1/e^2$ -radius via intermediate population of the  $^1D_2$  state where the atoms spend on average 10 ms. During this process the atoms remain subjected to magnetic trapping since the  $^1D_2$  state itself provides a trap potential with  $2/3$  of the size of that of the  $^3P_2$  state. If the initial atomic sample is smaller than the equilibrium distribution inside the magnetic trap, an expansion occurs which reduces the mean kinetic energy of the initial sample  $k_B T_i$  by the average potential energy of the final equilibrium distribution  $\rho$  minus the average potential energy of the initial distribution. Thus, for the quadrupole potential  $U$  the final kinetic energy is calculated to be  $k_B T_f = k_B T_i/3 + 0.172 \times \sigma \times U_0$ . The second term corresponds to 90  $\mu$ K for SMOT loading and may be neglected as compared to typical initial SMOT temperatures of 3 mK. Thus, temperatures above 1 mK are expected, exceeding the observed 0.6 mK. In case of TMOT loading in trace (2) a similar deviation is found. Here  $0.172 \times \sigma \times U_0$  amounts to 108  $\mu$ K and thus the expected temperature is 169  $\mu$ K as compared to 134  $\mu$ K observed.

Let us next estimate the capture efficiencies beginning with SMOT loading. We first calculate the average Zeeman detuning  $\delta_B$  experienced by the different Zeeman components of the  $^1P_1$  fraction of the SMOT sample in the quadrupole field  $U(x,y,z)$ . With  $b=26$  Gauss/cm we get  $\delta_B(m_J)/\Gamma = 0.08 \times m_J$ . Using these Zeeman detunings we calculate the average relative excitation probabilities of the  $^1P_1$  Zeeman components finding 37 % for the high field seeking  $m_J=-1$  state, 34 % for the non-magnetic state, and 29 % for the low field seeking  $m_J=1$  state. With the help of the Clebsch-Gordan coefficients we derive the relative populations of the Zeeman sub-levels in the  $^1D_2$  and  $^3P_2$  states respectively. We find 18 % population in the  $m_J=2$ , and 19 % population in the  $m_J=1$  low field seeking component of the  $^3P_2$  level

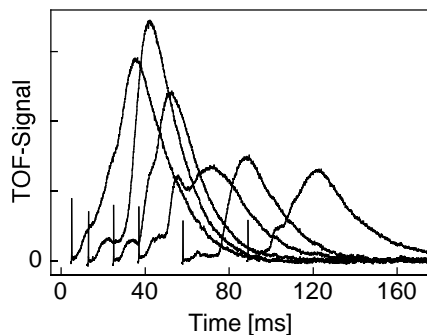


FIG. 4: TOF spectra for TMOT loading and short trapping durations (from left to right: 5 ms, 13 ms, 25 ms, 37 ms, 58 ms, 89 ms).

which are the two trapped states. In case of TMOT loading all atoms leaving the  $^1P_1$  state should be captured in the TMOT and about 20 % of those atoms should be transferred to each of the two magnetically trapped Zeeman sublevels. For SMOT loading only a fraction of the magnetically trapped atoms can contribute to the 657 nm fluorescence peak following the optical pumping pulse. In order to calculate the transfer efficiency by optical pumping we have numerically integrated the product of the thermal equilibrium distribution in the  $^3P_2$  potential  $\rho(x, y, z) = (32\pi)^{-1}(U_0/k_B T)^3 \exp(-U(x, y, z)/k_B T)$  and the local optical pumping probability during the 0.5 ms pumping pulse. To derive the local pumping probability we have solved a rate equation including all levels involved and account for the local intensity, polarization and the Zeeman detunings from resonance due to the magnetic quadrupole field. Temperatures are inserted as obtained from Fig.3b. For SMOT loading we find that a fraction of 39 % of the  $m_J=2$  atoms and 14 % of the  $m_J=1$  atoms is transferred. For TMOT loading no loss should occur in the optical pumping transfer.

For SMOT loading we typically observe a 657 nm fluorescence peak with  $2.9 \times 10^7$  atoms. Accounting for the

expected transfer efficiency by optical pumping discussed in the previous paragraph we obtain  $5.4 \times 10^7$  trapped  $m_J=2$  atoms and  $5.7 \times 10^7$  trapped  $m_J=1$  atoms. Assuming thermal equilibrium at 611  $\mu\text{K}$ , the peak density is  $3.4 \times 10^8 \text{cm}^{-3}$  for  $m_J=2$  atoms and  $1 \times 10^8 \text{cm}^{-3}$  for  $m_J=1$  atoms. Accounting for the loading time of 240 ms a capture rate of the  $m_J=2$  component of  $3.6 \times 10^8 \text{s}^{-1}$  is observed. This is to be compared with 18 % of the overall transfer rate of  $1.9 \times 10^{10} \text{s}^{-1}$ , i.e.  $3.4 \times 10^9 \text{s}^{-1}$ . For TMOT loading we find  $2.4 \times 10^8$  fluorescing atoms, and accordingly  $1.2 \times 10^8$  atoms in each of the two magnetically trapped Zeeman sublevels. Assuming thermal equilibrium at 135  $\mu\text{K}$ , we find a peak density of  $6.7 \times 10^{10} \text{cm}^{-3}$  for  $m_J=2$  atoms and  $2 \times 10^{10} \text{cm}^{-3}$  for  $m_J=1$  atoms. The observed  $m_J=2$  capture rate is  $7.9 \times 10^8 \text{s}^{-1}$  and has to be compared with 20 % of the overall transfer rate of  $1.9 \times 10^{10} \text{s}^{-1}$ , i.e.  $3.8 \times 10^9 \text{s}^{-1}$ . Presently, we cannot resolve the discrepancies between the expected and the observed capture rates which amount to a factor 9.4 for SMOT loading and a factor 4.8 for TMOT loading.

In summary, we have applied magnetic trapping to the group of earth alkaline atoms, preparing several times  $10^8$  calcium atoms in the  $^3P_2$  metastable state at peak densities near  $10^{11} \text{cm}^{-3}$  and temperatures around 0.13 mK. This represents favorable starting conditions for the formation of a metastable calcium BEC. Technical improvements (e.g. an extra transient cooling phase in the TMOT scheme, as explained in ref. [4], or a simple decrease of the background pressure) promise at least an order of magnitude improvement of the initial phase space density.

#### Acknowledgments

This work has been supported in part by the Deutsche Forschungsgemeinschaft (SPP 1116), DAAD probral/bu, and the European training network CAUAC.

- 
- [1] H. Katori, T. Ido, Y. Isoya, and M. Kuwata-Gonokami, Phys. Rev. Lett. **82**, 1116-1119 (1999).
  - [2] T. Binnewies *et al.*, Phys. Rev. Lett. **87**, 123002 (2001).
  - [3] E. A. Curtis, C. W. Oates, and L. Hollberg, Phys. Rev. A **64**, 031403(R) (2001).
  - [4] J. Grünert, and A. Hemmerich, Phys. Rev. A **65**, 041401(R) (2002).
  - [5] T. Kisters, K. Zeiske, F. Riehle, and J. Helmcke, J. Appl. Phys. B **59**, 89 (1994).
  - [6] F. Ruschewitz *et al.*, Phys. Rev. Lett. **80**, 3173 (1998).
  - [7] C. Oates, F. Bondu, R. Fox, and L. Hollberg, Eur. Phys. J. D. **7**, 449 (1999).
  - [8] T. P. Dinneen, K. R. Vogel, E. Arimondo, J. L. Hall, and A. Gallagher, Phys. Rev. A **59**, 1216 (1999).
  - [9] M. Machholm, P. S. Julienne, and K.-A. Suominen, Phys. Rev. A **64**, (2001).
  - [10] A. Derevianko *et al.*, <http://xxx.lanl.gov/abs/physics/0210076> (2002).
  - [11] M. H. Anderson *et al.*, Science **269**, 198 (1995).
  - [12] J. Grünert, G. Quehl, V. Elman, and A. Hemmerich, J. Mod. Opt. **47**, 2733 (2000); J. Grünert and A. Hemmerich, J. Appl. Phys. B **73**, 1-4 (2000).
  - [13] N. Beverini, F. Giammanco, E. Maccioni, F. Strumia, and G. Vissani, J. Opt. Soc. Am. B **6**, 2188-2193 (1989).
  - [14] T. Loftus, J. Bochinski, and T. Mossberg, Phys. Rev. A **66**, 013411 (2002).
  - [15] J. Stuhler *et al.*, Phys. Rev. A **64**, 031405 (2001).